JOINT INSTITUTE FOR NUCLEAR RESEARCH
Laboratory of Radiation Biology

FINAL REPORT ON THE START PROGRAMME

"Research on nanoparticles distribution in cancer cells for neutron capture therapy"

Supervisor:
Dr. Ermuhammad Dushanov

Student:
Yan Carlos Diaz Rodriguez, Cuba
Center for Advanced Studies of Cuba

Participation period:
August 06 – September 30,
Summer Session 2023

Dubna, 2023

Abstract

Boron neutron capture therapy (BNCT) is a promising cancer treatment that utilizes the interaction between boron-10 and thermal neutrons to produce alpha particles and lithium ions, which can selectively kill cancer cells. To enhance the efficacy of BNCT, various boron delivery agents have been developed, among which magnetite nanoparticles have gained increasing attention due to their unique magnetic properties and biocompatibility. Magnetic nanoparticles based on Fe_3O_4 and their modifications of surface with therapeutic substances are of great interest, especially drug delivery for cancer therapy includes boron-neutron capture therapy. Magnetic nanoparticles can be functionalized with boron-containing molecules and targeted to cancer cells using external magnetic fields, leading to high accumulation of boron in tumor tissues and improved treatment outcomes. This article will discuss the use of magnetite in BNCT and its potential as a promising strategy for cancer therapy.

Introduction

Boron neutron capture therapy is promising method for cancer treatment based on selective accumulation of boron-rich compound inside the cells and its neutron irradiation. It has shown promising results in the treatment of various types of cancer, including brain tumors, head and neck cancers, and melanoma [1-4]. The therapy involves the administration of a boron-containing compound, followed by the irradiation of the tumor with thermal neutrons. When the boron atoms absorb the neutrons, they undergo nuclear fission and release high-energy particles, such as alpha particles and lithium ions, which can selectively damage cancer cells while sparing healthy tissues.

One of the most widely used boron compounds in BNCT is *boronophenyilalanine* (BPA). BPA is a boron-containing amino acid that has been shown to accumulate preferentially in cancer cells, making it an attractive candidate for BNCT. However, one of the main challenges in BNCT is achieving high levels of boron accumulation in tumor tissues while minimizing the uptake in normal tissues. This requires the development of boron delivery agents that can specifically target cancer cells and enhance boron uptake. Overall, magnetite nanoparticles hold great promise as a delivery system for BNCT [5]. Their unique magnetic properties and biocompatibility make them an attractive option for targeted cancer therapy, and further research is needed to optimize their design and improve their clinical translation.

A first consideration in assessing magnetic nanoparticles (MNPs) toxicity as well as efficiency of translocation in a cell is the interaction of the MNPs with the cell membrane. Molecular dynamics (MD) simulations can provide insights into the interactions between boron-containing compounds and biological molecules, as well as the stability and efficacy of boron-containing nanoparticles for use in boron neutron capture therapy. Additionally, MD simulations can aid in the design and optimization of boron-containing compounds and nanoparticles for targeted delivery to cancer cells.

In the present work, MD simulations were performed to investigate the MNPs and boron compounds in contact with a model cell membrane in order to gain insights into the physicochemical properties that govern the interactions between them. Initially, a generic code that builds the model of the NP core of a given size and surface architecture was developed.

Boron neutron capture therapy

Boron neutron capture therapy is promising method for cancer treatment based on selective accumulation of boron-rich compound inside the cells and its neutron irradiation. Boron compounds and neutrons collide and cause atomic fission, producing a-Ray radiation, as the result, the cancer cells destroy from the inside [6].

After thermal neutron capture (Figure 1A), nonradioactive isotope ^{10}B releases alpha (^{4}He) particles and lithium nuclei (^{3}Li) (Figure 1B). These large energy transfer (LET) particles have very short range (<10 μm), comparable to the size of a single cell. Therefore, only one cell is destroyed by this reaction. Also, if boron is selectively taken up by the tumor cells, then it can kill tumor cells with less damage to normal cells [7] (Figure 1C). For a successful BNCT, there should be a high tumor uptake of ^{10}B (~20–100 μg/g or ~109 atoms/cell) and a low uptake of normal cells. The boron concentration ratio tumor: normal cells is usually recommended to be more than 3–4: 1. [8, 9]

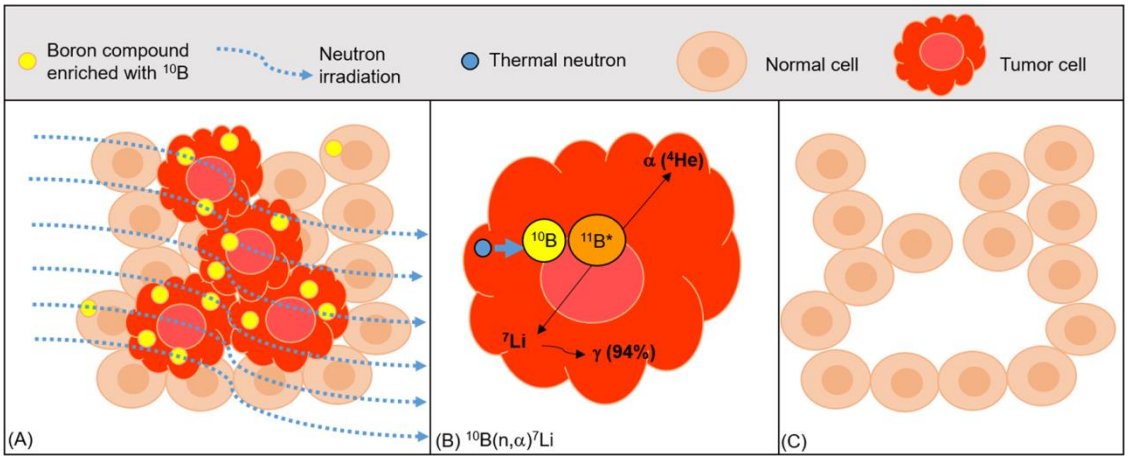

Figure 1: Schematic presentation of boron neutron therapy (BNCT). BNCT could selectively damage tumor cells while sparing normal ones as a targeted radiotherapy [10].

The most important BNCT limitation is low selectivity of such compounds. Different carries can be applied include magnetic NPs to increase the selective accumulation in tumorous tissues [10,11]. The main requirements for the nanostructures use as containers for targeted drug delivery are: the possibility of transporting drugs directly to the affected tissues or organs, reducing side effects, carrier non-toxicity and stability. Presently, there are two boron compounds that are used clinically, p-boronophenylalanine (BPA) and borocaptate sodium (BSH).

Materials and Methods

Boron Compounds

BNCT provides a tool to selectively destroy malignant cells when a sufficient amount of is selectively delivered to the tumor with sufficient thermal neutron fluence from an external radiation source [12, 13].

Boron agents used in BNCT would ideally:

- Be able to maintain the ^{10}B-concentration in tumor tissues to a level at which an antitumor effect can be anticipated during neutron irradiation;
- Have systemic toxicity low enough to ensure safety. Furthermore, while achieving higher uptake into the tumor tissue than the normal tissue, the ratios "concentration in tumor tissue / concentration in normal tissue" (T/N) and "concentration in tumor tissue /concentration in blood" (T/B) have to be high;
- Be rapidly cleared from normal tissues and blood after neutron irradiation;
- Comply with the guidelines for neoplastic agents of the International Council for Harmonisation of Technical Requirements for Pharmaceuticals for Human Use.

Boronophenylalanine

One of the most widely used boron compounds in BNCT is boronophenylalanine (BPA). It is a boron-containing amino acid that has been shown to accumulate preferentially in cancer cells, making it an attractive candidate for BNCT. BPA is administered intravenously and is taken up by cancer cells through the same mechanism as phenylalanine, an essential amino acid. Once inside the cancer cell, the boron atoms in BPA are selectively taken up and accumulate in the tumor tissue.

- The development of the application of BPA in BNCT is outlined below:
- 1989: the potential for treating melanomas with BPA was first demonstrated
- 1999: BPA was used for treatment of malignant brain tumors
- 2001: the first extracorporeal liver BNCT treatment of diffuse metastases using BPA was performed
- 2004: the first BNCT treatment of head and neck cancers with both BPA and BSH in combination using epithermal neutrons was performed. Within a couple of years, the effectiveness of BNCT with BPA alone was confirmed in the treatment of locally recurrent head and neck cancer
- 2020: BPA in use with AB-BNCT was approved for treating locally recurrent head and neck cancer in Japan [14].

Borocaptate sodium

Mercapto-undecahydro-closo-dodecaborate (borocaptate sodium or BSH), is an icosahedral, dianionic, water soluble boron anion cluster composed of 12 boron atoms, was developed in the

late 1960s [14]. In 1975, BSH was the first boron agent to demonstrate a significant antitumor effect in BNCT of malignant brain tumors [15] from treatments that began in 1968.

Although BSH has a low selectivity for cancer cells, it has high water solubility and low toxicity. In a healthy brain, water soluble substances in blood are sparingly taken up by normal brain tissue due to the presence of the blood–brain barrier. However, in brain tumors, disruption to the blood–brain barrier permits the entry and accumulation of water-soluble compounds in brain tissue. Thus, BSH is considered to be accumulated in brain tumors.

Other boron compounds, such as boron carbide (B4C), have also been investigated for their potential use in BNTC. These compounds offer unique advantages and challenges in terms of their pharmacokinetics, tumor selectivity, and toxicity profiles [16].

Magnetic Nanoparticles (MNPs)

Nanoparticles (NPs) as drug delivery systems are engineered technologies for the delivery of therapeutic agents to their targets in a controlled manner and have shown significant potential to be employed in cancer treatment, with the aim to improve the biodistribution of cancer drugs. Magnetic nanoparticles (MNPs) are a class of nanoparticles, which can be manipulated using magnetic field gradients in order to reach the target site of interest and deliver the drug faster and more efficiently. Common MNPs consist of biocompatible iron oxide MNPs such as magnetite (Fe3O4) and its oxidized form maghemite (γ-Fe 2O3) with proper surface architecture and conjugated targeting ligands/proteins.

They can be functionalized with various molecules, including boron-containing compounds, to enable targeted delivery to cancer cells (Figure 2). When exposed to an external magnetic field, the nanoparticles can be directed to specific regions of the body, such as tumor tissues, where they can accumulate and release the boron compound upon neutron irradiation. Several studies have demonstrated the potential of magnetite nanoparticles in enhancing the efficacy of BNCT [17].

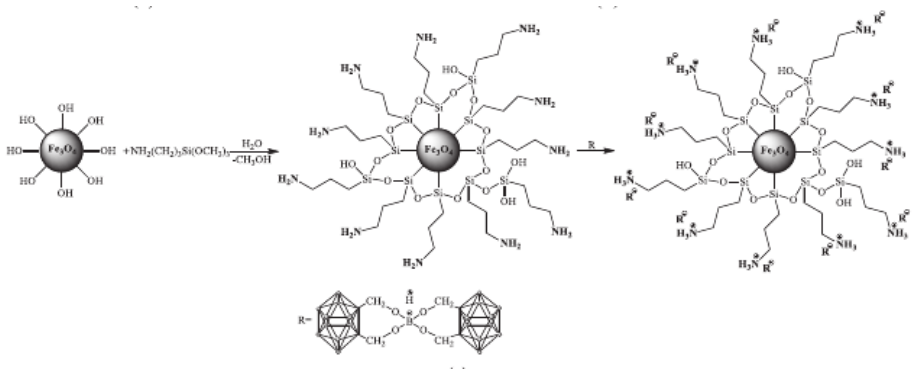

Figure 2: Schematic representation of carborane derivatives immobilization on Fe_3O_4 [17].

Membrane lipid bilayer

The membrane lipid bilayer is a thin, flexible barrier that surrounds and separates the contents of a cell from its external environment. It is composed of two layers of phospholipid molecules, which have a hydrophilic (water-loving) head and a hydrophobic (water-fearing) tail. The hydrophilic

heads face outward, interacting with the aqueous environment inside and outside the cell, while the hydrophobic tails face inward, interacting with each other to form a stable, impermeable barrier. The membrane lipid bilayer also contains various proteins and other molecules that help to regulate the movement of substances in and out of the cell.

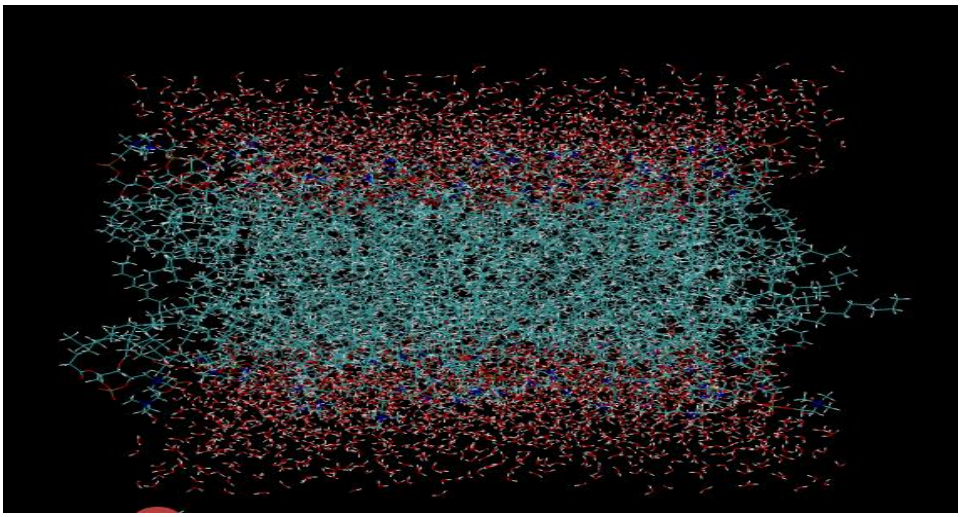

Figure 3: Representation of the POPC lipid bilayer in Visual Molecular Dynamics.

The membrane lipid bilayer that we simulate in this work is composed of phospholipid molecules, including POPC (1-palmitoyl-2-oleoyl-sn-glycero-3-phosphocholine), which is a commonly found phospholipid in cell membranes (Figure 3). The hydrophilic head of POPC contains a choline group, a glycerol molecule, and a phosphate group, while the hydrophobic tail consists of a saturated palmitoyl chain and an unsaturated oleoyl chain (Figure 4). These phospholipids self-assemble into a bilayer, with the hydrophilic heads facing outward and the hydrophobic tails facing inward, forming a stable barrier that separates the contents of the cell from its external environment.

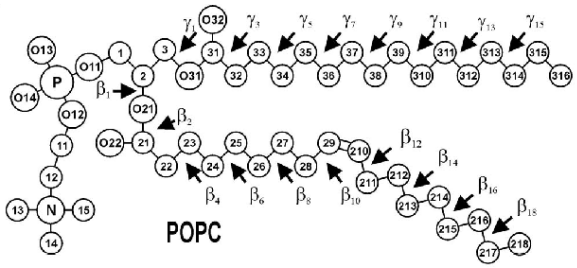

Figure 4: Molecular structure with numbering of atoms and torsion angles of POPC.

MD simulations

Molecular dynamics (MD) simulations are a computational technique that uses classical mechanics to study the motions and interactions of atoms and molecules over time. In MD simulations, the behavior of a system is modeled by solving the equations of motion for each atom in the system, taking into account the forces that act on them. The resulting trajectories can then be analyzed to gain insights into the behavior of the system.

Molecular dynamics simulations are a powerful computational tool that can be used to model the behavior of boron-containing compounds and nanoparticles in biological systems. These simulations can provide valuable insights into the interactions between boron-containing compounds and biological molecules, such as proteins and DNA. By simulating the motion and behavior of individual atoms and molecules over time, molecular dynamics simulations can help researchers understand how boron-containing compounds interact with their biological targets, and how these interactions affect the efficacy of boron neutron capture therapy.

One important application of molecular dynamics simulations in boron neutron capture therapy is in the design and optimization of boron-containing nanoparticles for targeted delivery to cancer cells. By simulating the behavior of these nanoparticles in different biological environments, researchers can gain insights into how to optimize their size, shape, and surface properties to improve their ability to target cancer cells. Additionally, molecular dynamics simulations can be used to evaluate the stability and toxicity of these nanoparticles, helping to ensure their safety for use in clinical applications. We use GROMACS software for MD simulations.

GROMACS

GROMACS (GROningen MAchine for Chemical Simulations) is a widely used molecular dynamics simulation software that is designed to simulate the behavior of biological molecules such as proteins, lipids, and nucleic acids. It is a free and open-source software suite for high-performance molecular dynamics and output analysis**.** It is a versatile package to perform molecular dynamics, i.e., simulate the Newtonian equations of motion for systems with hundreds to millions of particles [18].

GROMACS is specifically designed for MD simulations of biomolecules, and it includes a range of features that make it particularly useful for this purpose. For example, it includes a range of force fields that are specifically tailored to different types of biomolecules, as well as a range of tools for preparing and analyzing simulation data. Its support for a range of simulation protocols, including energy minimization, equilibration, and production runs. Also includes a range of tools for analyzing simulation data, such as trajectory analysis tools and visualization tools. Overall, it is a powerful and versatile tool for studying the behavior of biomolecules using molecular dynamics simulations [19].

CHARMM

CHARMM (Chemistry at HARvard Molecular Mechanics) is a highly versatile and widely used molecular simulation program. It has been developed over the last three decades with a primary focus on molecules of biological interest, including proteins, peptides, lipids, nucleic acids, carbohydrates and small molecule ligands, as they occur in solution, crystals, and membrane environments. For the study of such systems, the program provides a large suite of computational tools that include numerous conformational and path sampling methods, free energy estimators, molecular minimization, dynamics, and analysis techniques, and model-building capabilities. In addition, the CHARMM program is applicable to problems involving a much broader class of many-particle systems. Calculations with CHARMM can be performed using a number of different energy functions and models, from mixed quantum mechanical-molecular mechanical

force fields, to all-atom classical potential energy functions with explicit solvent and various boundary conditions, to implicit solvent and membrane models [20].

CHARMM-GUI, http://www.charmm-gui.org, has been developed to provide a web-based graphical user interface to generate various input files and molecular systems to facilitate and standardize the usage of common and advanced simulation techniques in CHARMM. The web environment provides an ideal platform to build and validate a molecular model system in an interactive fashion such that, if a problem is found through visual inspection, one can go back to the previous setup and regenerate the whole system again [21].

Ambertools and ACPYPE

AmberTools consists of several independently developed packages that work well by themselves, and with Amber itself. The suite can also be used to carry out complete molecular dynamic simulations, with either explicit water or generalized Born solvent models. It contains packages/tools to generate force fields for general organic molecules and metal centers, preparation programs for Amber simulations, semi-empirical and DFTB quantum chemistry program, tools to perform numerical solutions to Poisson-Boltzmann models, programs for structure and dynamics analysis of trajectories, etc. [22].

ACPYPE (or AnteChamber PYthon Parser interfacE) is a wrapper script around the ANTECHAMBER software that simplifies the generation of small molecule topologies and parameters for a variety of molecular dynamics programs like GROMACS, CHARMM and CNS. It is written in the Python programming language and was developed as a tool for interfacing with other Python based applications such as the CCPN software suite (for NMR data analysis) and ARIA (for structure calculations from NMR data). ACPYPE is open-source code, under GNU GPL v3, and is available as a stand-alone application at http://www.ccpn.ac.uk/acpype and as a web portal application at http://webapps.ccpn.ac.uk/acpype [23].

Visual Molecular Dynamics

Visual Molecular Dynamics (VMD) is a molecular graphics program designed for the display and analysis of molecular assemblies, in particular biopolymers such as proteins and nucleic acids. VMD can simultaneously display any number of structures using a wide variety of rendering styles and coloring methods. It provides a complete graphical user interface for program control and has also been expressly designed with the ability to animate MD simulation trajectories [24].

Construction of the magnetite nanoparticle

Magnetite has a crystallographic cubic inverse spinel form. The oxygen ions form a close-packed cubic network with the iron ions situated at interstices among the oxygen ions. Two variations of interstices that the metal ions are able to form are identified, the tetrahedral (A) sites and the octahedral (B) sites (Figure 5) [25].

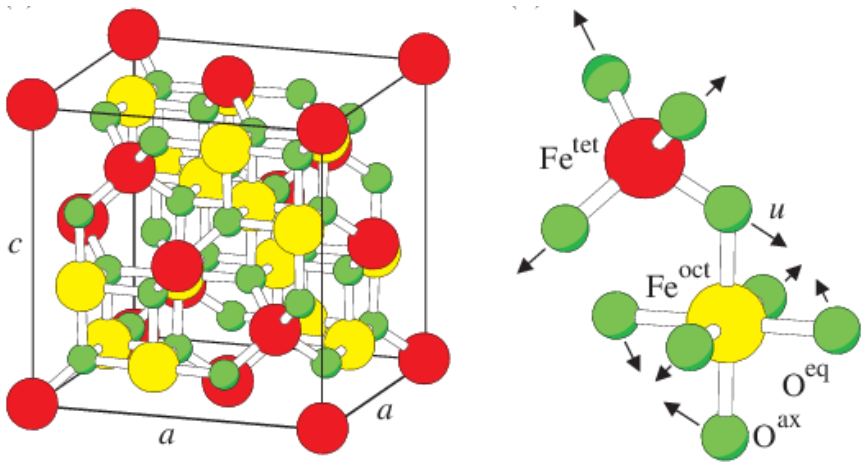

Figure 2: Face-centered cubic inverse spinel structure of magnetite.

Higher than 120K A sites are occupied by Fe^{3+} ions only and the B sites by both Fe^{3+} and Fe^{2+} ions, with double the B sites occupied than A sites. At any given moment (in the scale of 1 nanosecond) the B sites are occupied by either a Fe^{3+} or a Fe^{2+} ion. In this study, the unit cell of the magnetite crystal is downloaded from the crystallography open database (http://www.crystallography.net/) [26] with CIF number 1011032. It consists of 56 atoms with unit cell parameters a=b=c=8.39 Å and its space group is the Fd-3m.

The first step, after visualizing the unit cell of the magnetite (Figure 6a), is to replicate it in the xyz direction to construct a spherical nanoparticle by using crystallographic tool for the construction of nanoparticles Nano Crystal [27]. So that the size of the replicated crystal to be 25 Å of diameter (Figure 6b).

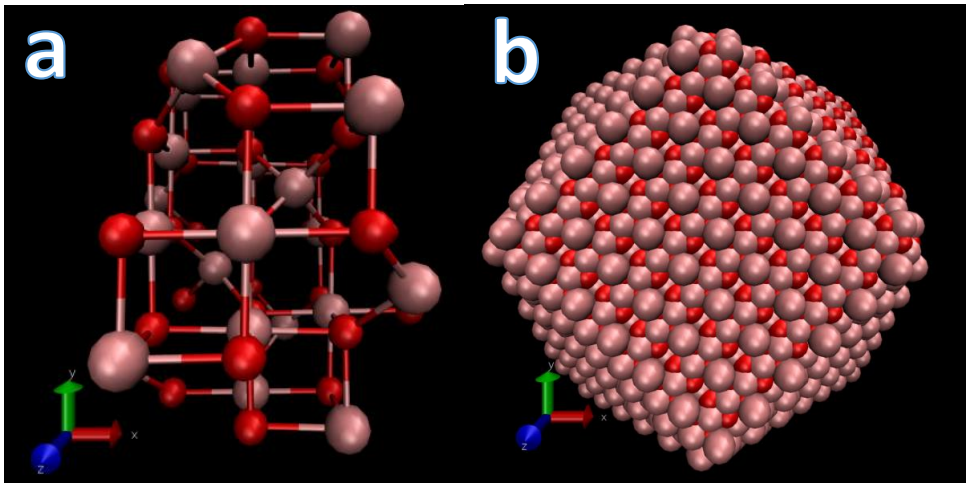

Figure 3: Representation of the (a) unit cell and (b) nanoparticle of magnetite in Visual Molecular Dynamics.

Gromacs topology

For running our Molecular Dynamics Simulations using Gromacs simulation package, version 2022.4, topology files including information for the magnetite core and the two types of molecular chains are needed.

Topology information include partial charges, bond lengths of bonded atoms and their force constants along with their atomic indexes. The same information is needed for their angles and the dihedral angles that are formed. The Fe^{2+}, Fe^{3+} and O^{2-} have partial charges 1.54, 1.76 and -1.21 respectively [28]. In order all lengths and angles of bonded atoms to be defined, the magnetite unit cell is the starting point as its values are repeated for the whole structure.

Construction of the Boron compounds

4-Borono-L-phenylalanine

The structures files for the BPA ligand (Figure 7) were extracted from the structure of p-boronophenylalanyl tRNA synthetase in complex with p-boronophenylalanine and adenosine monophosphate (5N5U) with ID ligand: 7N8 downloaded from RCSB Protein Data Bank web site (https://www.rcsb.org) [29].

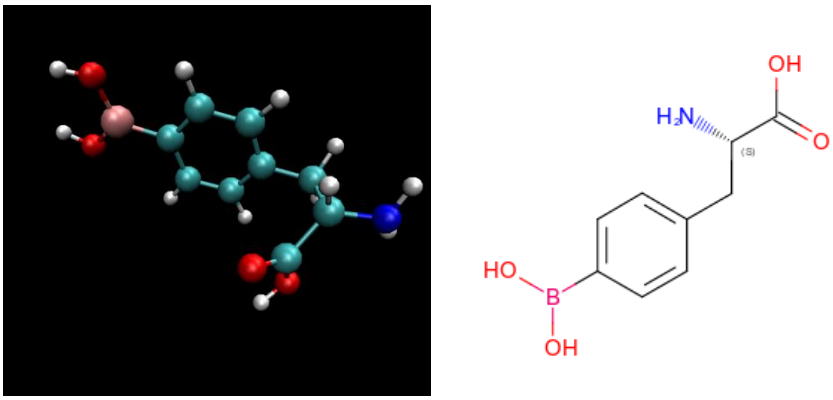

Figure 4: Representation of the structure of a BPA molecule (Boron atoms in pink).

Borocaptate sodium

The structure files for the BSH ligand (Figure 8) were extracted from the structure of Hen egg white lysozyme with boron trace drug UTX-97 (5B5J) with ID ligand: UTX downloaded from RCSB Protein Data Bank web site (https://www.rcsb.org) [29]. The molecule was parametrized with the help of acpype software in Gaff Force Field from Ambers. The topology was built with Ambertools.

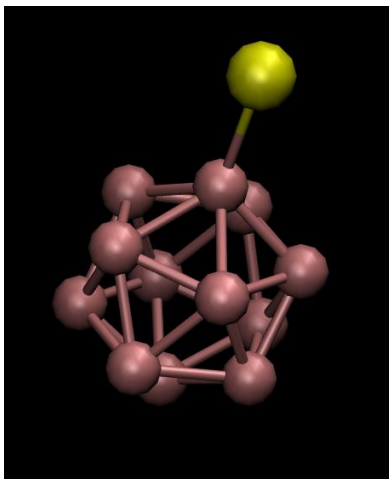

Figure 5: Representation of the structure of a BSH molecule (Boron atoms in pink).

Boron carbide (B4C)

The B4C nanoparticles (Figure 9) were built in the extension Ligand Reader & Modeler corresponding to the web-based graphical user interface CHARMM-GUI who generate various ligand structures using the CHARMM force field [21].

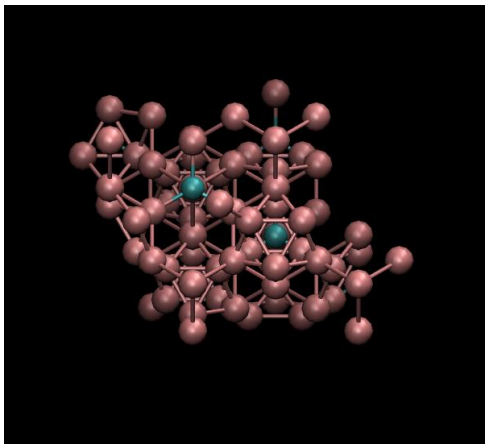

Figure 9: Representation of the structure of a B4C molecule in VMD (Boron atoms in pink).

Boron nitride nanotubes (BNNTs)

The BNNTs were built in Boron Nitride Nanostructure Builder Plugin which is part of the VMD Extensions (Figure 10). This plugin allows construction of boron nitride nanostructures like single-wall nanotubes or graphene-like sheets [24]. The nanotube length was of 5 nm and the values of the chiral index n and m were 5 and 10 respectively.

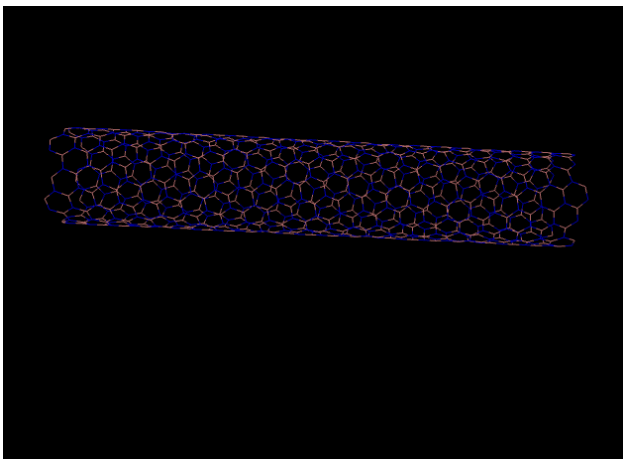

Figure 10: Representation of the structure of a BN nanotube in VMD.

Molecular Dynamics simulations

Molecular Dynamics simulations using GROMACS 2022.4 package were performed using 242 POPC lipid bilayer (121 POPC in each leaflet) and 12100 water molecules. 27 water molecules were replaced by cations in K^{1+} and additional 27 water molecules were replaced by Cl^{1-} counter ions to neutralize the charge. Bilayer leaflets were placed at a water slab with lipid headgroups oriented toward the water phase. To simulate the interaction of the membrane and boron compounds were used two molecules of PBA and four molecules of BSH. The box of a rectangular prismatic shape was employed with periodic boundary conditions applied in all directions. The initial topology for BPA was taken from literature. The web-based graphical user interface CHARMM-GUI, http://www.charmm-gui.org, were used to generate the input files for running the minimization, equilibration and simulation of the molecular dynamics. Also, Amber Tool and CPYPE software were used to parametrize the BSH molecules and built their topologies. Visual Molecular Dynamics 1.9.4 (VMD) was used for the production of snapshots.

Modeling was carried out in three stages:

i) minimization of the energy;
ii) NVT and NPT equilibration of the system; and
iii) molecular dynamics (MD) calculations with the CHARMM36 force field and General Amber Force Field (Gaff)

The average deviation of lipid membrane thickness (DM), area per lipid (AL), radial distribution functions, and deuterium parameter order were calculated using the GROMACS auxiliary program.

Production

The initial configurations produced by CHARMMGUI were not suitable for being directly used as input for a NVT simulation. Therefore, an energy minimization was performed after packing for all the systems, using a steepest-decent algorithm the energy minimizations converged after 1210 steps for BPA+membrane system and 1218 steps for BSH+membrane system. The resulting structures were then equilibrated in two steps shorts NVT simulations of 250 ps at a temperature

of 303.15 K using periodic boundary conditions in all directions. These general parameters were used in all equilibration and production runs. The integration of the equations of motion was performed using a leap-frog algorithm (GROMACS integrator md). Initial velocities assigned to the beads were randomly taken from a normal distribution for the corresponding temperature. To keep the membrane in the middle of the simulation box, the center-of-mass motion was removed in every step of this first equilibration. The following options were used:

• A time step of 1 fs was chosen for better energy conservation

• A cut-off of 2.0 nm for van-der-Waals interactions with a force-switch that, starting at 0.9 nm, smoothly brings the value of the potential to zero at the cutoff distance

• The particle-mesh Ewald (PME) method for calculation of electrostatic interactions

In all equilibrations a V-rescale thermostat with a bath temperature of 303.15 K and a coupling constant of 1 ps was used. Lipids, water molecules and nanoparticles each had separated groups for temperature-coupling. Subsequently the resulting structures were used as input for an NPT simulation in four steps for another 1000 ps (4x250 ps). The simulation parameters were almost identical to the ones in the NVT equilibration. As only difference semiisotropic pressure coupling was added while the volume of the simulation box was freed. A C-rescale barostat was used in the equilibration with a reference pressure of 4.5 bar, a coupling constant of 5.0 ps and a compressibility of 1. After the NPT equilibration, the states of the equilibrated systems were investigated by use of the GROMACS *gmx energy* analysis tool. The temperature, box lengths in x, y and z direction, average density as well as the energies for bonds, angles, Lennard-Jones and Coulomb interactions were calculated. With these results the equilibrations were considered successful for all systems.

Results and Discussion

BPA/BSH – membrane molecular dynamics simulation

To ensure that the system reach the equilibrium we obtain the *root mean square deviation* for the Phosphorus atoms in the lipid bilayer. The root-mean-square deviation of atomic positions, or simply root-mean-square deviation (RMSD), is the measure of the average distance between the atoms (usually the backbone atoms). The Figure 11 shows how the system reaches an equilibrium after 80 ns for the BPA system and after 40 ns for the BHS system.

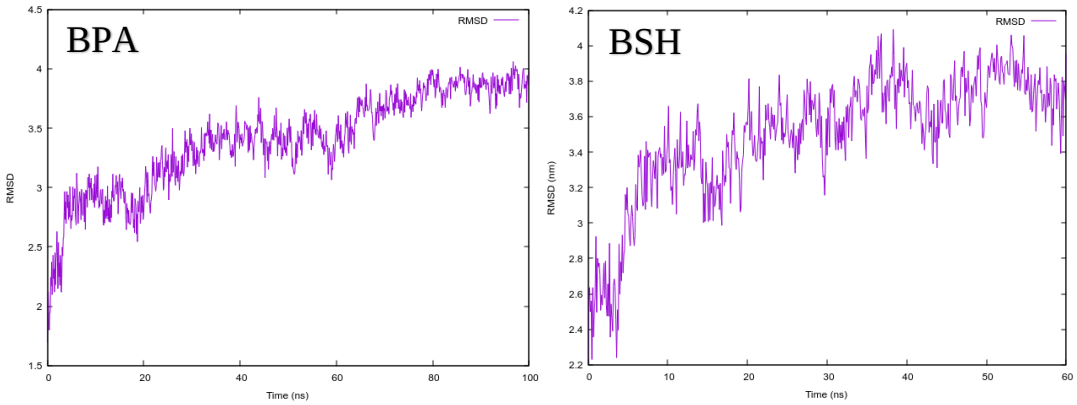

Figure 11: RMSD calculation for the phosphorus atoms in the membrane during the time of the simulation for BPA and BSH ligands.

The *membrane thickness* characterizes the transverse structure of the membrane. It constitutes an essential property of the bilayer that in turn modulates membrane functionality, like the hydrophobic mismatch affecting integral protein functionality. The *membrane thickness* strongly depends on the lipid composition.

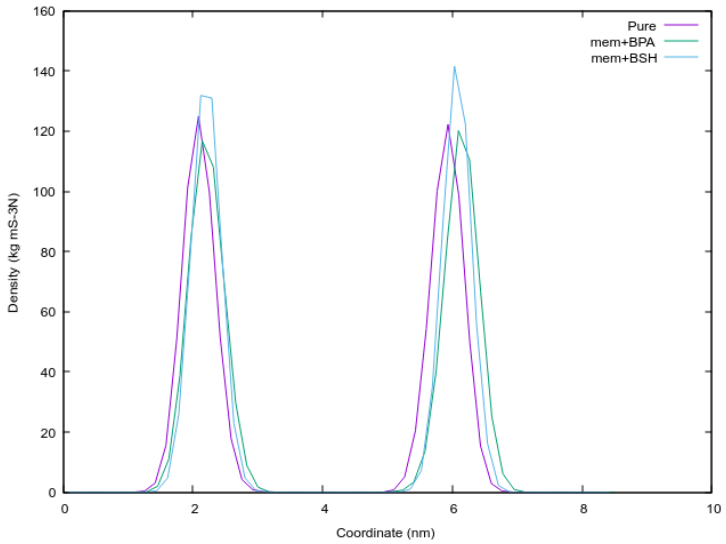

Figure 12: Density profile of the phosphorus atoms in the bilayer.

The thickness bilayer was defined as the average distance between the phosphate atoms in the two monolayers (Figure 12). Changes in the headgroup, length, or unsaturation level of the acyl chains are reflected in its value. In this case the POPC membrane thickness did not change significantly as we can see in Table 1. The higher value obtained from the system with BPA compared to the system with BSH may be due to the greater internalization of the BPA molecules in the membrane.

	Bilayer thickness (nm)	Error (nm)	Area/lipid (nm2)	Error (nm2)
Pure membrane	3,826	0.012	0.643	0.016
BPA-membrane	3,930	0.012	0.639	0.025
BSH- membrane	3.865	0.012	0.641	0.023

Table 1: Dynamical properties values obtained for both systems.

The *area per lipid* (APL) in a pure bilayer corresponds to the total average membrane area divided by the number of lipid molecules in a single leaflet. It is a basic variable that characterizes the bilayer structure, and its value depends significantly on the membrane composition, hydration level of the membrane, ionic force of the medium, pH, temperature and pressure. Its value summarizes large amounts of structural and dynamic properties of the membrane and is a clear indicator of the membrane's phase and is often used in validation of the particular lipid force field.

The *area per lipid* a was calculated with the Gromacs tool *gmx energy* by simply dividing the area of our simulation box by half the number of lipids in our system. The area per lipids is slightly reduced by the effect of the interaction (Table 1) between the ligands and the membrane and for the pure POPC membrane is in agreement with previously reported experimental findings [30,31].

Other important parameter to obtain in this kind of systems is the *membrane density profile*. It is the time average of some extensive property of the system along the z-direction, the one perpendicular to the bilayer plane. Typically measured properties are mass, electronic density, charge, scattering length, occurrence, etc. Membrane *density profiles* are interesting as they can be obtained experimentally as well as from MD simulations. Although different experimental techniques provide access to different profiles, here the attention is focused on mass electron density profiles as we can see in Figure 13.

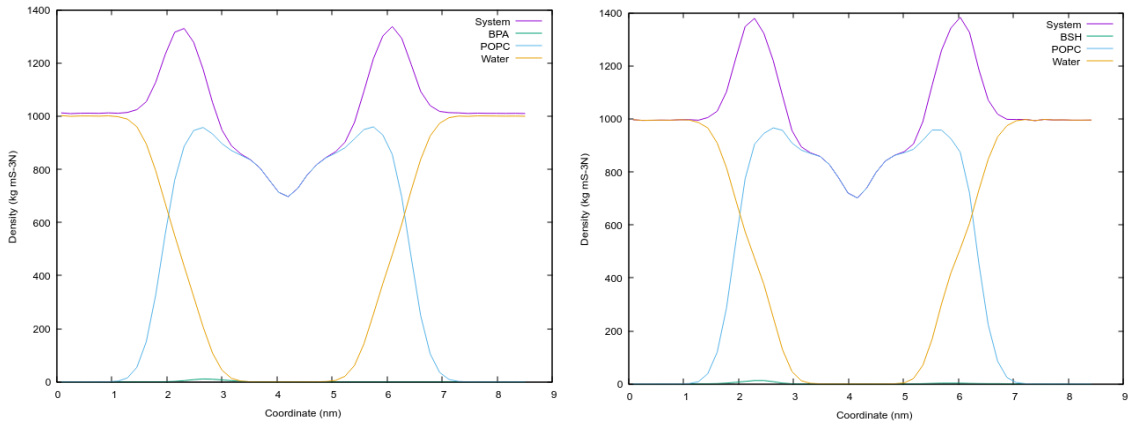

Figure 136: Density profiles for all the system and each component.

The *density profile* confirms the visual assessment of the equilibrium positions of the BPA and the BSH ligands as it is shown in Figure 13. It is interesting how our atomistic simulations indicates that both, BPA and BSH bind spontaneously to the membrane, as can be seen in Figure 14 and 15.

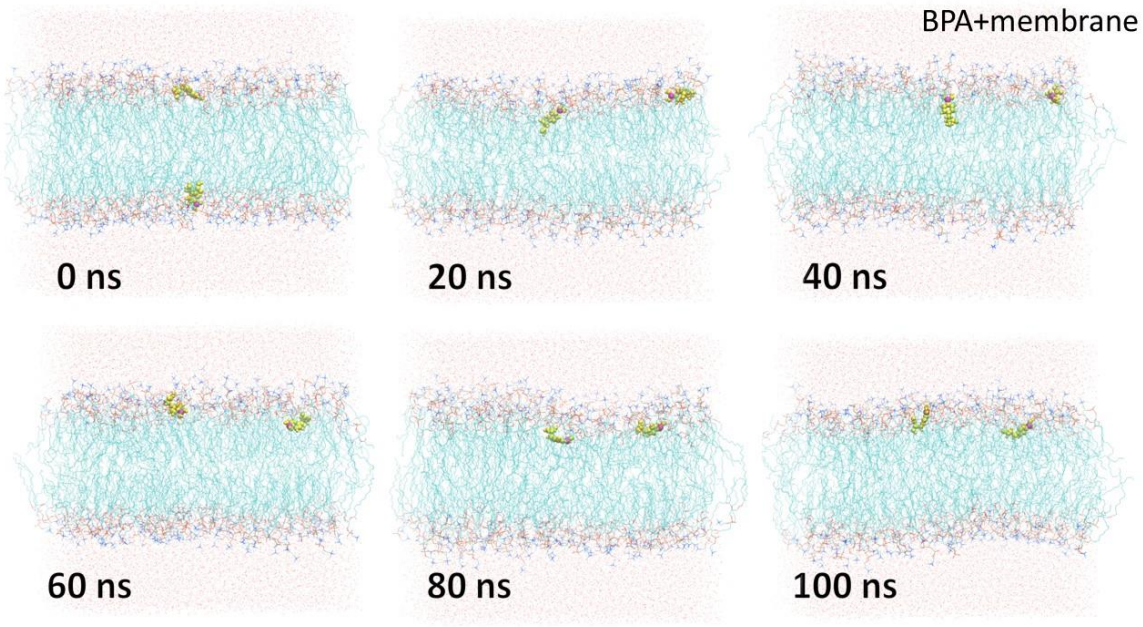

Figure 14: Images of the system BPA+membrane in different steps of the simulation represented in VMD.

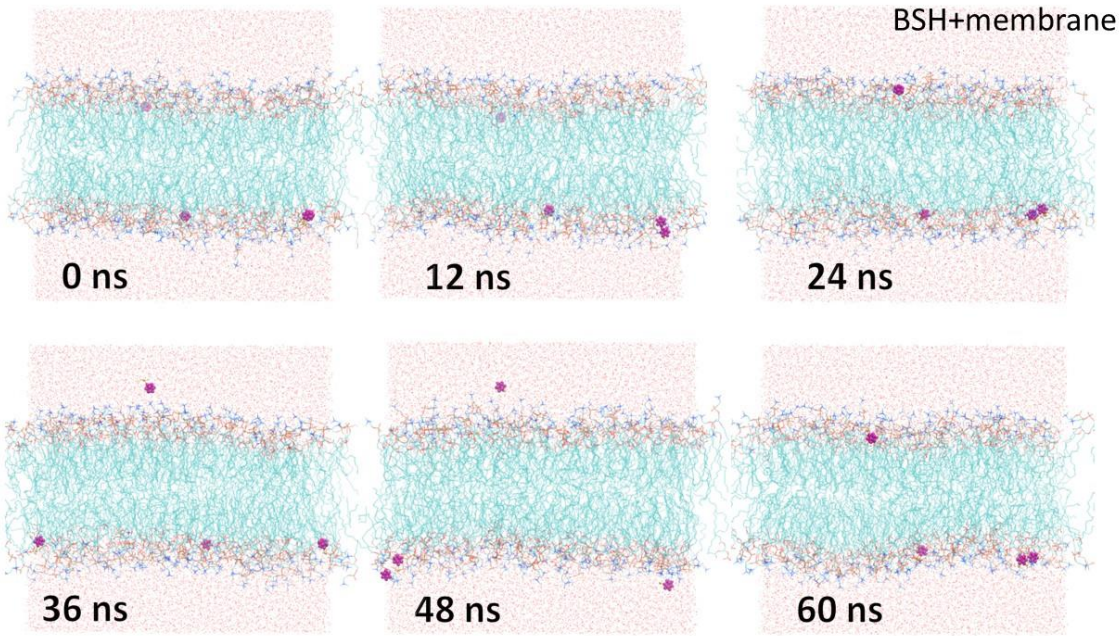

Figure 15: Images of the system BSH+membrane in different steps of the simulation represented in VMD.

Figure 16 shows the progress of the distance between Boron from BPA (a)/BSH (b) and the phosphate group heads of the lipids in the membrane. The minimum distance of contacts between the BPA and the membrane keeps lower than 1 nm of distance (of the order of the molecule's length) and tends to a stability around 4 Å. Something similar happens for the BSH system, being the minimum contact distance below the 6 Å. This result indicates that the direct contacts of ligands with the lipid membrane components are negligible.

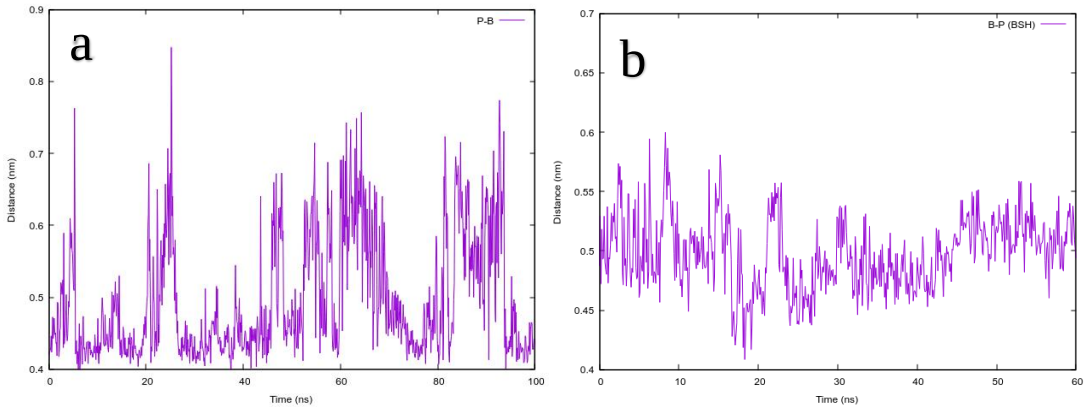

Figure 16: Number of contacts between the boron in the BPA molecule and phosphorus on the membrane.

The fluid nature of the membrane, due to the balance between the attractive intermolecular interaction and the disordering thermal motion, is shown by the nonexistence of a well-defined (solid-like) positional ordering. Despite this, membranes in their fluid phase still display certain levels of spatial ordering. The analysis of this ordering allows for the identification and description of the fundamental interactions between membrane components that are responsible for the final membrane structure. This analysis is usually performed using a *radial distribution function (RDF)* which describes the structure of a system as the variation in particle number density with distance from a reference particle. According to the $g(r)$ plots (Figure 17), the interactions between BPA (a) and the atoms from the phospholipid's heads are crucial at shorts distances suggesting a kind of bond between them. First peaks of B-N and B-P orders are located at 0.42 nm and 0.48 nm, respectively. For the BSH this interaction (b), this interaction occurs at a greater distance, evidencing less link behavior. In this case, first peaks are located at 0.55 nm and 0.56 nm.

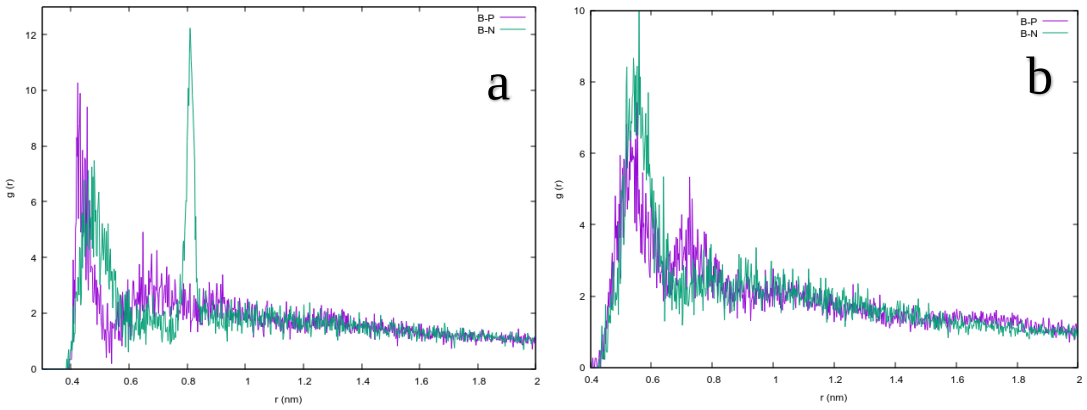

Figure 17: Radial Distribution Function calculated for the interaction of boron with the lipid heads.

The *deuterium order parameter* S_{CD} which provides an idea on how ordered is an acyl chain at the chosen segment. The S_{CD} is defined as:

$$S_{CD} = \frac{1}{2}\langle 3\cos^2(\theta) - 1\rangle$$

where θ y is the angle between the Carbon–Deuterium bond and the bilayer normal, and the angular brackets denote averaging over time and over all phospholipids.

To directly investigate the ordering effect of the BPA and BSH ligands on the phospholipid acyl tails, the *deuterium order parameter* of the lipid tails was computed for each carbon in the two chains (Figure 18). The S_{CD} for pure saturated lipids can be directly compared with the order parameter measured in NMR experiments [32]. The simulated order parameters for the lipid sn-1 (palmitic acid) and sn-2 (oleic acid) segments agree very well with the corresponding experimental results for the pure POPC membrane.

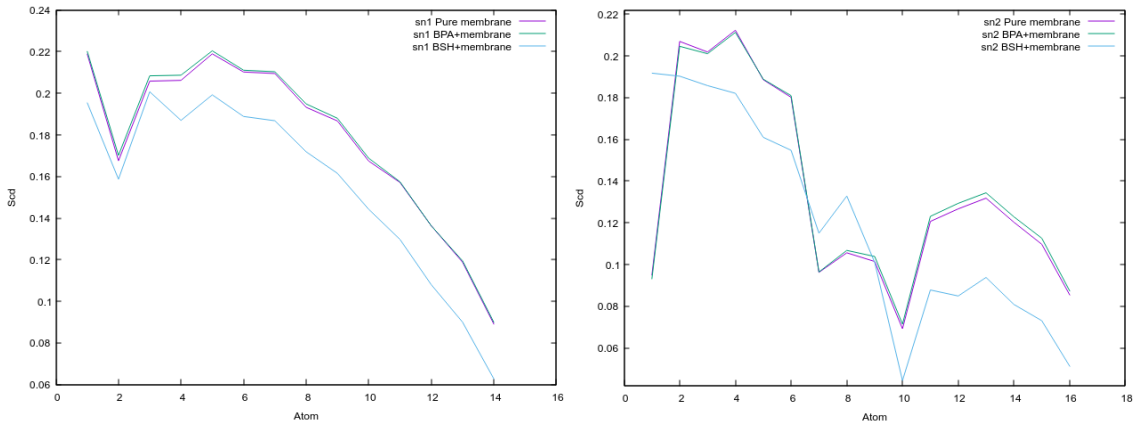

Figure18: Profile of the deuterium order parameter (SCD) for sn-1 (a) and sn-2 (b) chains of POPC molecule at the different studied systems.

It can be clearly observed how there were practically no changes in the deuterium order parameter for the system with BPA with respect to the pure POPC bilayer membrane. On the contrary, in the case of the system with BSH, very evident changes occurred mainly in the first carbons of the sn2 chain (oleic acid). These changes could be due to the type of interaction that exists between BSH and the membrane, which differs from the mechanism by which BPA interacts.

Conclusions

Development of the world's computing allows the scientist to perform molecular dynamics simulation on hundreds of or thousands of atoms with computer. Molecular dynamics simulation is a technique for investigating structure of atoms based on the interaction with other atoms.

The aim for this study was build a POPC bilayer and the analysis of their interaction with different nanoparticles by molecular dynamics simulation for BNCT. Four boron-based structure of nanoparticles was obtained by different methods and a MNPs of magnetite was built to use as drug carrier in this kind of therapy.

Atomistic-level structural properties of the POPC bilayer interacting with a BPA and BSH ligands were investigated by a simulation in GROMACS software. The analysis of the results confirm that the membrane does not undergo significant changes as a result of this interaction. It also reveals that the ligands tend to spontaneously bind to the surface of the membrane composed of a glycerol molecule, choline and a phosphate groups.

MD calculations showed that BPA can penetrate into the cell/nucleus membrane. Such effect can lead to the lethal destruction of tumor cells during BNCT. In addition, it was observed that there is a slight affinity of the membrane to the Boronphenylaline nanoparticle with respect to Borocaptate Sodium, which agrees with the studies carried out on these compounds previously in boron electron capture therapy.

Recommendations and future work

It is recommended as future work to obtain the topology of the other boron compounds that were not simulated in this study and of the magnetite nanoparticle using the necessary parameters in the construction of the force field corresponding to each of them.

Acknowledges

This project is prepared in fulfilment of the requirement for the START program at JINR. I owe my deepest gratitude to the research group at Laboratory of Radiation Biology, Joint Institute of Nuclear Research for providing me with an opportunity through the START program to work on this project. I also extend my gratitude towards my project supervisor and mentor, Dr Ermuhammad Dushanov whose guidance and expertise have been invaluable in steering me towards success.

Bibliography

1. Kato I, Fujita Y, Maruhashi A, Kumada H, Ohmae M, Kirihata M, Imahori Y, Suzuki M, Sakrai Y, Sumi T, Iwai S, Nakazawa M, Murata I, Miyamaru H, Ono K. Effectiveness of boron neutron capture therapy for recurrent head and neck malignancies. Appl Radiat Isot. 2009 Jul;67(7-8 Suppl): S37-42. doi: 10.1016/j.apradiso.2009.03.103. Epub 2009 Apr 2. PMID: 19409799.

2. Barth RF, Vicente MG, Harling OK, Kiger WS 3rd, Riley KJ, Binns PJ, Wagner FM, Suzuki M, Aihara T, Kato I, Kawabata S. Current status of boron neutron capture therapy of high-grade gliomas and recurrent head and neck cancer. Radiat Oncol. 2012 Aug 29;7:146. doi: 10.1186/1748-717X-7-146. PMID: 22929110; PMCID: PMC3583064.

3. Yong Z, Song Z, Zhou Y, Liu T, Zhang Z, Zhao Y, Chen Y, Jin C, Chen X, Lu J, Han R, Li P, Sun X, Wang G, Shi G, Zhu S. Boron neutron capture therapy for malignant melanoma: first clinical case report in China. Chin J Cancer Res. 2016 Dec;28(6):634-640. doi: 10.21147/j.issn.1000-9604.2016.06.10. PMID: 28174492; PMCID: PMC5242447.

4. Kankaanranta L, Seppälä T, Koivunoro H, Välimäki P, Beule A, Collan J, Kortesniemi M, Uusi-Simola J, Kotiluoto P, Auterinen I, Serèn T, Paetau A, Saarilahti K, Savolainen S, Joensuu H. L-boronophenylalanine-mediated boron neutron capture therapy for malignant glioma progressing after external beam radiation therapy: a Phase I study. Int J Radiat Oncol Biol Phys. 2011 Jun 1;80(2):369-76. doi: 10.1016/j.ijrobp.2010.02.031. Epub 2011 Jan 13. PMID: 21236605.

5. Oleshkevich E, Morancho A, Saha A, Galenkamp KMO, Grayston A, Crich SG, Alberti D, Protti N, Comella JX, Teixidor F, Rosell A, Viñas C. Combining magnetic nanoparticles and icosahedral boron clusters in biocompatible inorganic nanohybrids for cancer therapy. Nanomedicine. 2019 Aug; 20:101986. doi: 10.1016/j.nano.2019.03.008. Epub 2019 May 3. PMID: 31059794.

6. Monti Hughes A. Importance of radiobiological studies for the advancement of boron neutron capture therapy (BNCT). Expert Rev Mol Med. 2022 Mar 31;24: e14. doi: 10.1017/erm.2022.7. PMID: 35357286.

7. Suzuki, M., 2020. Boron neutron capture therapy (BNCT): a unique role in radiotherapy with a view to entering the accelerator-based BNCT era. Int. J. Clin. Oncol. 25, 43–50.

8. Barth, R.F., Mi, P., Yang, W., 2018. Boron delivery agents for neutron capture therapy of cancer. Cancer Commun. 38, 35.

9. Miyatake, S., Kawabata, S., Hiramatsu, R., Kuroiwa, T., Suzuki, M., Kondo, N., Ono, K., 2016. Boron neutron capture therapy for malignant brain tumors. Neurol. Med.-Chir. 56, 361–371. Naga Ch, P., Gurram, L., Chopra, S., Mahantshetty, U., 2018. The management of locally

10. A. Chakrabarti, N.S. Hosmane, Pure Appl. Chem. 84 (2012) 2299.Y. Zhu, Y. Lin, Y.Z. Zhu, J. Lu, J.A. Maguire, N.S. Hosmane, J. Nanomater. 2010 (2010) 112.
11. SOLOWAY, A.H., et al., The chemistry of neutron capture therapy, Chem. Rev. 984 (1998) 1515–1562.

12. BARTH, R.F., CODERRE, J.A., VICENTE, M.G., BLUE, T.E., Boron neutron capture therapy of cancer: Current status and future prospects, Clin. Cancer Res. 11 11 (2005) 3987–4002.

13. INTERNATIONAL ATOMIC ENERGY AGENCY, Advances in Boron Neutron Capture Therapy, Non-serial Publications, IAEA, Vienna (2023), ISBN 978–92–0–132623–2

14. HATANAKA, H., A revised boron-neutron capture therapy for malignant brain tumors, J. Neurol. 209 2 (1975) 81–94.

15. D.I. Tishkevich, *et all*. Boron neutron capture therapy anti-tumor effect of nanostructured boron carbon nitride: A new potential candidate. Inorganic Chemistry Communications Volume 157, November 2023, 111318

16. Tietze R, Unterweger H, Dürr S, Lyer S, Canella L, Kudejova P, Wagner FM, Petry W, Taccardi N, Alexiou C. Boron containing magnetic nanoparticles for neutron capture therapy--an innovative approach for specifically targeting tumors. Appl Radiat Isot. 2015 Dec; 106:151-5. doi: 10.1016/j.apradiso.2015.07.028. Epub 2015 Jul 26. PMID: 26242559.

17. Van Der Spoel D, Lindahl E, Hess B, Groenhof G, Mark AE, Berendsen HJ. GROMACS: fast, flexible, and free. J Comput Chem. 2005 Dec;26(16):1701-18. doi: 10.1002/jcc.20291. PMID: 16211538.

18. https://www.gromacs.org/

19. Brooks BR et all. CHARMM: the biomolecular simulation program. J Comput Chem. 2009 Jul 30;30(10):1545-614. doi: 10.1002/jcc.21287. PMID: 19444816; PMCID: PMC2810661.

20. Jo S, Kim T, Iyer VG, Im W. CHARMM-GUI: a web-based graphical user interface for CHARMM. J Comput Chem. 2008 Aug;29(11):1859-65. doi: 10.1002/jcc.20945. PMID: 18351591.

21. D.A. Case, H.M. *et all* (2023), Amber 2023, University of California, San Francisco.

22. Sousa da Silva, A.W., Vranken, W.F. ACPYPE - AnteChamber PYthon Parser interfacE. BMC Res Notes 5, 367 (2012). https://doi.org/10.1186/1756-0500-5-367

23. Humphrey, W., Dalke, A. and Schulten, K., VMD — Visual Molecular Dynamics // J.
24. Molec.Graphics, 1996, 14.1, 33-38.

25. Friák, Martin & Schindlmayr, Arno & Scheffler, Matthias. (2007). Ab initio study of the half-metal to metal transition in strained magnetite. New J. Phys. 9. 10.1088/1367-2630/9/1/005.

26. Crystallography Open Database (COD), http://www.crystallography.net/

27. https://nanocrystal.vi-seem.eu/CrystalTool/index.php

28. T. Manz, D. Sholl; Chemically Meaningful Atomic Charges That Reproduce the Electrostatic Potential in Periodic and Nonperiodic Materials; J. Chem. Theory Comput. 2010, 6, 2455–2468.

29. https://www.rcsb.org

30. N. Kučerka, S. Tristram-Nagle, J.F. Nagle, Structure of fully hydrated fluid phase lipid bilayers with monounsaturated chains, J. Membr. Biol. 208 (3) (2006) 193–202, http://dx.doi.org/10.1007/s00232-005-7006-8.

31. N. Kučerka, M.-P. Nieh, J. Katsaras, Fluid phase lipid areas and bilayer thicknesses of commonly used phosphatidylcholines as a function of temperature, Biochim. Biophys. Acta Biomembr. 1808 (11) (2011) 2761–2771, http://dx.doi.org/10. 1016/j.bbamem.2011.07.022.

32. J. Seelig, N. Waespe-Sarcevic, Molecular order in cis and trans unsaturated phospholipid bilayers, Biochemistry 17 (16) (1978) 3310–3315, http://dx.doi.org/10. 1021/bi00609a021.